ELSEVIER

C 1s and O 1s photoelectron spectra of formaldehyde with satellites: theory and experiment[☆]

K. Kuramoto[a], M. Ehara[a], H. Nakatsuji[a,b,*], M. Kitajima[c],
H. Tanaka[c], A. De Fanis[d], Y. Tamenori[d], K. Ueda[e]

[a] *Department of Synthetic Chemistry and Biological Chemistry, Graduate School of Engineering, Kyoto University,
Kyoto-Daigaku-Katsura, Nishikyou-ku, Kyoto 615-8510, Japan*
[b] *Fukui Institute for Fundamental Chemistry, Kyoto University, 34-4 Takano-Nishihiraki-cho, Sakyo-ku, Kyoto 606-8103, Japan*
[c] *Department of Physics, Sophia University, Tokyo 102-8854, Japan*
[d] *SPring-8/JASRI, Sayou-gun, Hyogo 679-5198, Japan*
[e] *Institute of Multidisciplinary Research for Advanced Materials, Tohoku University, Sendai 980-8577, Japan*

Available online 5 November 2004

Abstract

Shake-up satellite spectra accompanying the C 1s and O 1s photoelectron main lines of formaldehyde were studied by the combination of high-resolution X-ray photoelectron spectroscopy and accurate ab initio calculations. The symmetry adapted cluster–configuration interaction (SAC–CI) general-R method finely reproduced the details of the experimental spectra and enabled quantitative assignments for the seven satellite bands: some were newly interpreted. The shake-up transitions were mainly attributed to the valence excitations accompanying the inner-shell ionization. The Rydberg excitations were found to be minor. Three-electron processes such as $1s^{-1}n^{-2}\pi^{*2}$ and $1s^{-1}\pi^{-2}\pi^{*2}$ were predicted in the low-energy region where the valence shake-up states such as $1s^{-1}n$–σ^*, π–π^* exist.
© 2004 Elsevier B.V. All rights reserved.

Keywords: C 1s and O 1s photoelectron spectra; Formaldehyde; Shake-up satellite, SAC-CI

1. Introduction

Shake-up satellites appearing in the inner-shell photoelectron spectra are challenging spectroscopic subject from both theory and experiment. Theoretically, a proper description of the satellite spectra is possible only with advanced accurate theoretical methods, since the spectra reflect very complex electron-correlation and orbital-reorganization effects. Experimentally, weak intensities of the inner-shell photoelectron satellites make high-resolution X-ray photoelectron spectroscopy (XPS) difficult. Recently, studies of the inner-shell photoelectron satellites invoked renewal of interest, because significant developments in both high-resolution XPS and accurate theoretical methods have made us possible to obtain precise knowledge and assignments of the satellite spectra accompanying the inner-shell main lines. This situation has further motivated intensive cooperative researches on the shake-up states associated with the inner-shell ionization, from both experimental and theoretical sides.

Inner-shell photoelectron satellite spectra of molecules were measured extensively around 1970 [1,2]. A spectrum of formaldehyde was first recorded by Carroll and Thomas [3] and investigated theoretically by Basch [4] with the ab initio multi-configuration SCF (MC-SCF) method and by Hillier and Kendrick with the RHF method [5]. Later, the spectrum was recorded at higher resolution and the observed band structures were assigned with the help of the semi-empirical INDO-CI calculations [6]. The Green's function method, algebraic diagrammatic construction (ADC) (4), was also applied to the calculations of the inner-shell photoelectron satellite spectrum up to ∼17 eV [7] relative to the inner-shell main line energy. The result was encouraging for the C 1s photoelectron satellite spectrum, whereas it was not

sufficient for the O 1s photoelectron satellite spectrum: the contribution from the 3h2p configurations turned out to be significant in the latter spectrum. There are still some discrepancies between theory and experiment and so the natures of the band structures have not yet been fully understood. Furthermore, the contributions from the Rydberg excitations have not been theoretically examined. Thus, intensive cooperative investigations by high-resolution XPS and an accurate theoretical method are necessary for elucidating fine details of the shake-up satellite spectra accompanying the C 1s and O 1s main line of formaldehyde.

In the present work, the C 1s and O 1s photoelectron satellite spectra of formaldehyde are measured by means of high-resolution XPS and analyzed in details by means of the symmetry adapted cluster (SAC) [8]/SAC-configuration interaction (CI) method [9,10]. This theoretical method has been established as a reliable and useful tool for investigating a variety of spectroscopy through many successful applications [11–15]. We use here the SAC–CI general-R method [16–18], which has been designed to describe multiple-electron processes with high accuracy. This method has been shown to be useful for clarifying the fine details of the satellite peaks appearing in the valence photoemission spectra of molecules [19,20]. Recently, we have systematically applied the general-R method to the core-level photoemission and provided accurate results for the core electron binding energies (CEBEs) of molecules and further the satellite spectra of CH_4, NH_3 [21] and H_2O [22,23]. Formaldehyde has n–π^*, π–π^* and Rydberg excitations accompanying the inner-shell photoemission and therefore the inner-shell photoelectron satellite spectra are much more characteristic and complex in contrast to those of CH_4, NH_3 and H_2O.

2. Experimental

The experiments were conducted at the c-branch of the soft X-ray photochemistry experiments beamline 27SU [24] at SPring-8, the 8 GeV synchrotron radiation facilities in Japan. The monochromator installed in this beam line is of Hettrick type and a high-resolution between 10 000 and 20 000 can be achieved [25,26]. Another notable feature of the beamline is a figure-8 undulator [27] as a light source, with which we can perform the angle-resolved electron spectroscopy. This undulator serves a useful function to switch the direction of the polarization vector from horizontal to vertical, and vice versa, only by varying the gap of the undulator. The degree of light polarization was confirmed to be better than 0.98 for both directions by the measurement of the 2s and 2p photoelectrons of Ne. The electron spectroscopy apparatus of Gamma Data Scienta makes equipped also on the beamline, consists of a hemispherical electron analyzer (SES-2002) with a Herzog-plate termination and accelerating-retarding multi-element lens as well as with a gas-cell (GC-50), which are installed in the differentially pumped chamber [28]. A combination of this electron spectroscopy apparatus and the state-of-the-

art soft X-ray beamline provides us excellent opportunity of performing high-resolution XPS [22,23,29,30].

In the present measurements, the C 1s and O 1s photoelectron satellite spectra of formaldehyde were recorded at photon energies 400 and 650 eV, respectively, with experimental overall resolutions of $\Delta E = 220$ meV at 400 eV and $\Delta E = 290$ meV at 650 eV, respectively. The formaldehyde (H_2CO) in its dimerized form, i.e., *para*-formaldehyde, was purchased commercially from WAKO, Japan, with a stated purity of 97%, and was degassed simply by repeated freeze under the pressure of ($\sim 10^{-4}$ Pa) without further purification. The formaldehyde target beam was prepared directly from the *para*-formaldehyde by heating a bottle containing the solid to 50–65 °C. At this temperature, a background pressure of $\sim 10^{-4}$ Pa (uncorrected for the ionization efficiency of formaldehyde) was measured in the experimental chamber, in which the gas-cell is placed. A plug of glass wool was placed over the powder in the reservoir to prevent the powder from dispersing during warming or pumping of the reservoir. All tubing from the reservoir to the gas-cell were heated to ~ 60 °C to prevent condensation and possible polymerization of the formaldehyde vapor in the inlet lines. Moreover, the whole electron spectrometer apparatus was kept at ~ 65 °C during the measurement. Assuming equilibrium conditions apply, the dimer/monomer ratio was estimated to be $\leq 10^{-4}$ under the experimental conditions ($\sim 10^{-4}$ Pa H_2CO pressure and ~ 50 °C) and thus the contribution from the dimer could be neglected.

3. Computational details

We study here the vertical ionization processes and therefore the molecular geometry was fixed to the experimental one [31]. We used the extensive basis sets to allow the description of the orbital reorganization and electron correlations that are important in the present study; i.e., triple zeta (VTZ) (10s6p)/[6s3p] Gaussian type orbitals (GTOs) for C and O [32], augmented with two polarization d-functions [33], and Rydberg functions [2s2p2d] [34]. For H atom, the VTZ (6s1p)/[3s1p] set was used. The resultant basis sets were [8s5p4d/3s1p].

We use the SAC–CI general-R method to describe the C 1s and O 1s core ionization and the shake-up satellite spectra. We used different sets of R operators for C 1s and O 1s ionizations but the core–hole valence separation approximation was not adopted. We studied the satellites dominantly described by doubles with considerable contribution of triples and therefore, we included the R operators up to quadruples in the general-R calculation. All MOs were included in the active space to describe core–hole relaxation.

To reduce the computational requirements, the perturbation selection procedure was adopted [35]. Reference functions for selections were chosen from the small-active-space SDT-CI vectors to guarantee the accuracy, at least, up to the three-electron processes. The threshold of the linked terms

Table 1
The dimensions of the selected SAC–CI general-*R* operators for the *K*-shell ionized states of formaldehyde

	Singles	Doubles	Triples	Quadruples	Total
C 1s hole	5	317	26416	242009	268747
O 1s hole	5	336	23181	223767	247289

for the ground state was set to $\lambda_g = 5.0 \times 10^{-6}$ au and the unlinked terms were adopted as the products of the important linked terms whose SDCI coefficients were larger than 0.005. For the inner-shell ionized states, the thresholds of the linked terms, which are doubles and triples, were set at $\lambda_e = 5.0 \times 10^{-7}$ and those of the quadruples were set at 5.0×10^{-5}. The thresholds of the CI coefficients for calculating the unlinked operators in the SAC–CI method were 0.05 and 0.001 for the *R* and *S* operators, respectively. The dimensions of the selected SAC–CI linked operators employed were summarized in Table 1.

The ionization cross-sections were calculated using the monopole approximation [35] to estimate the relative intensities of the peaks. Both initial- and final-ionic-state correlation effects were included.

The SAC/SAC–CI calculations were executed with the Gaussian03 suite of programs [36] with some modifications for calculating the inner-shell ionization spectra.

4. Results and discussion

4.1. C 1s shake-up satellites

The observed spectrum and the SAC–CI general-*R* spectrum for the C 1s shake-up satellites are presented in Fig. 1. Experimentally, seven satellite bands 1–7 are numbered according to Ref. [6]. In the SAC–CI spectrum, the solid vertical lines indicate the calculated pole strengths: they were convoluted using Gaussians with the FWHM of 1.2 eV. The present XPS measurement gives high-resolution spectrum which
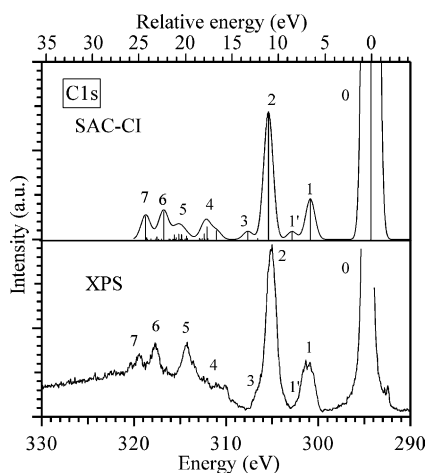
Fig. 1. C 1s photoelectron satellite spectrum of formaldehyde.

contains fine peak structures in some bands due to the vibrational progression and/or numerous satellite states, in comparison with the previous one [6]. Lunell et al. [6] reported both experimental and theoretical spectra of the inner-shell photoelectron emission of formaldehyde. Their INDO/CI calculations were, however, not sufficient for the detailed assignments of the bands. Table 2 summarizes the ionization energies relative to the main line, relative monopole intensities, and SAC–CI main configurations for the C 1s shake-up satellite states of formaldehyde. The CEBE of C 1s main line is calculated to be 294.30 eV, resulting in reasonable agreement with the experimental value of 294.47 eV. We have listed only the states whose relative intensities were larger than 0.0005: many other states with small intensities were not given.

As seen from Fig. 1, the agreement between theory and experiment is encouraging, though the intensity of the XPS does not necessarily agree with the theoretical monopole intensity. The first satellite band 1 was previously assigned to the shake-up state of the triplet $(\pi^{-1}\pi^*)$ parentage [5,7]. The present calculation confirms that the main contribution is from the triplet $(\pi^{-1}\pi^*)$ transition, while a fractional contribution from the Rydberg $(\pi^{-1}3p)$ excitation may not be negligible. The calculated energy of this state is 6.57 eV, in fair agreement with the observed value 6.4 eV. The calculated relative intensity is 0.0168, while the experimental values are between 0.005 and 0.010 [6]. According to the calculation, the equilibrium C−O bond length of this shake-up state is larger than that of the ground state [37] and therefore the fine peak structures observed for this band may be attributed mostly to the C−O vibrational components. Interestingly, the calculation predicts a band arising from the three-electron process $(n^{-2}\pi^{*2})$ at 8.55 eV, i.e., on the high-energy side of band 1. Its intensity is as small as 0.0033. The band is labeled as band 1' in Fig. 1. It may be possible that this state contributes to some fine peak structures of the band 1 on the high-energy side. Lunell et al. [6] also predicted the satellite band of this character at 7.25 eV with the intensity of 0.001. Their assignment was however different: they assigned band 1 to this three-electron process instead of $(\pi^{-1}\pi^*)$. The ADC(4) calculation predicted this doubly excited state at 12.21 eV and they mentioned this state should be placed lower by 3–4 eV [7].

The strongest band 2 was previously assigned to the shake-up state arising from the $(\pi^{-1}\pi^*)$ transition [5–7]. The present assignment is consistent with the other works. The calculated energy is, however, 11.11 eV, about 0.5 eV higher than the measured energy 10.6 eV. The difference is larger than 0.3 eV, which is usually the maximum deviation of SAC–CI from experiments. The calculation gives large relative intensity 0.0528 for this band, in agreement with the experiment. The fine peak structures observed for this band are attributed to the vibrational components, as in the case of band 1. On the high-energy side of this band, a small shoulder structure, labeled as band 3, was observed and previously assigned to the $(n^{-1}3b_2(\sigma^*))$ state [6]. This shoulder structure appears also in the present spectrum, at 12.2 eV. In our

calculation, two shake-up states dominantly characterized as $(n^{-1}3b_2(\sigma^*))$ are predicted at 12.29 and 13.34 eV, with the relative intensities of 0.0005 and 0.0034, respectively.

A complex band 4 centered at 16.3 eV is observed. Many shake-up states are predicted in this energy region, though their monopole intensities are small. This band is mainly attributed to a mixture of the three-electron process $(\pi^{-2}\pi^{*2})$ and the two-electron process $(5a_1(\sigma)^{-1}6a_1(\sigma^*))$ accompanying the C 1s ionization. In the region of band 5, we also predict several shake-up states with small intensities with the characters of $(\pi^{-1}3b_2(\sigma^*)n^{-1}\pi^*)$ and $(5a_1(\sigma)^{-1}6a_1(\sigma^*))$. The calculated energies are 20.55, 20.86, and 21.34 eV, whereas the calculated intensities are around 0.002. In the energy region of bands 4 and 5, many shake-up states of the Rydberg excitations such as $(n^{-1}3p)$ and $(n^{-1}4p)$ are predicted, although these transitions have very small intensities.

Band 6 observed at 23.3 eV can be attributed to the valence $(\pi^{-1}3b_2(\sigma^*))$ and Rydberg $(\pi^{-1}3d)$ mixed transition. The band 7 is characterized as a linear combination of the valence and Rydberg transitions, $(4a_1(\sigma)^{-1}6a_1(\sigma^*))$ and $(\pi^{-1}3d)$, and the three-electron valence process $(4a_1(\sigma)^{-2}\pi^{*2})$.

Thus, the shake-up satellite bands of the C 1s ionization of formaldehyde are mostly attributed to the valence excitations accompanying the core-ionization and the Rydberg excitations are predicted to have small contributions. The present calculations do not predict any shake-up satellite states with significant monopole intensities, in the energy region higher than band 7.

4.2. O 1s satellite spectrum of formaldehyde

The SAC–CI calculation results in the O 1s CEBE at 539.35 eV, in good agreement with the experimental value 539.48 eV. In Fig. 2, the calculated and observed spectra are compared and the band numbers are given according to the previous work [6]. Note that band 7 was missing in the previous experimental spectrum [6]. The present results of the O

Table 2
Ionization potential (IP) (eV), relative energy to the main line (ΔE) (eV), monopole intensity and main configurations of the C 1s satellite states of formaldehyde

No.	Lunell et al.[a] Experimental ΔE (eV)	Intensity	CISD/INDO ΔE (eV)	Intensity	This work Experimental IP (eV)	ΔE (eV)	Intensity	SAC-CI general-R IP (eV)	ΔE (eV)	Intensity	Main configurations[b] ($|C|>0.25$)
0	0.0	1.000	–	–	294.47	0.0	1.000	294.30	0.0	1.0000	$0.79\,(C\,1s^{-1}) - 0.29\,(\pi^{-1}\pi^*\,C\,1s^{-1})$
1	6.7	0.010	–	–	300.87	6.4	0.005	300.87	6.57	0.0168	$0.72\,(C\,1s^{-1}\pi^*\pi^{-1}) + 0.41\,(\pi^{-1}\pi^*\,C\,1s^{-1}) + 0.26\,(C\,1s^{-1}3p\pi^{-1})$
1'	–	–	7.25	0.001				302.85	8.55	0.0033	$0.78\,(n^{-1}\pi^*n^{-}\pi^*\,C\,1s^{-1}) + 0.30\,(n^{-1}3pn^{-1}3b_2(\sigma^*)\,C\,1s^{-1}) + 0.28\,(n^{-1}3b_2(\sigma^*)n^{-1}3p\,C\,1s^{-1})$
2	10.7	0.034	10.50	0.054	305.07	10.6	0.018	305.41	11.11	0.0528	$0.66\,(\pi^{-1}\pi^*\,C\,1s^{-1}) - 0.28\,(\pi^{-1}\pi^*\pi^{-}\pi^*\,C\,1s^{-1})$
3	12.2	0.004	11.60	0.005	306.67	12.2	0.002	306.59	12.29	0.0005	$0.71\,(C\,1s^{-1}3b_2(\sigma^*)\,n^{-1}) + 0.55\,(n^{-1}3b_2(\sigma^*)\,C\,1s^{-1})$
								307.64	13.34	0.0034	$0.46\,(n^{-1}3b_2(\sigma^*)\,C\,1s^{-1}) - 0.28\,(C\,1s^{-1}3b_2(\sigma^*)n^{-1})$
4	16.3	0.008	14.21	0.053	310.77	16.3	0.001	311.05	16.75	0.0036	$0.51\,(\pi^{-1}\pi^*\pi^{-1}\pi^*\,C\,1s^{-1}) - 0.35\,(n^{-1}\pi^*n^{-1}\pi^*\,C\,1s^{-1})$
								312.09	17.79	0.0051	$0.48\,(5a_1(\sigma)^{-1}6a_1(\sigma^*)\,C\,1s^{-1}) + 0.42\,(C\,1s^{-1}6a_1(\sigma^*)\,5a_1(\sigma)^{-1}) + 0.29\,(C\,1s^{-1}3dn^{-1})$
5	19.9	0.015	22.44	0.011	314.27	19.8	0.007	312.37	18.07	0.0024	$0.49\,(5a_1(\sigma)^{-1}6a_1(\sigma^*)\,C\,1s^{-1}) - 0.45\,(C\,1s^{-1}3dn^{-1}) + 0.37\,(C\,1s^{-1}4pn^{-1})$
								314.85	20.55	0.0020	$0.67\,(\pi^{-1}3b_2(\sigma^*)n^{-1}\pi^*\,C\,1s^{-1}) + 0.57\,(\pi^{-1}3b_2(\sigma^*)\,C\,1s^{-1}\pi^*n^{-1})$
								315.16	20.86	0.0022	$0.31\,(n^{-1}3b_2(\sigma^*)\,C\,1s^{-1}) + 0.29\,(1b_2(\sigma^*)^{-1}3b_2(\sigma^*)\,C\,1s^{-1})$
								315.64	21.34	0.0019	$0.48\,(5a_1(\sigma)^{-1}6a_1(\sigma^*)\,C\,1s^{-1}) - 0.32\,(\pi^{-1}3b_2(\sigma^*)n^{-1}\pi^*\,C\,1s^{-1})$
6	23.3	0.015	27.54	0.063	317.77	23.3	0.007	316.77	22.47	0.0115	$0.38\,(1b_2(\sigma^*)^{-1}3b_2(\sigma^*)\,C\,1s^{-1}) - 0.31\,(C\,1s^{-1}3d\pi^{-1}) + 0.25\,(\pi^{-1}\pi^*\,C\,1s^{-1})$
7	25.0	0.014	29.19	0.013	319.37	24.9	0.005	318.75	24.45	0.0094	$0.30\,(C\,1s^{-1}6a_1(\sigma^*)4a_1(\sigma)^{-1}) - 0.26\,(\pi^{-1}3d\,C\,1s^{-1}) + 0.24\,(4a_1(\sigma)^{-1}\pi^*\,4a_1(\sigma)^{-1}\pi^*\,C\,1s^{-1})$

[a] Ref. [6].
[b] The spin functions of doubles (iaj) and triples $(iajbk)$ are $\frac{1}{\sqrt{2}}(\alpha\beta - \beta\alpha)\alpha$ and $\frac{1}{2}(\alpha\beta - \beta\alpha)(\alpha\beta - \beta\alpha)\alpha$, respectively.

Fig. 2. O 1s photoelectron satellite spectrum of formaldehyde.

Table 3
Ionization potential (IP) (eV), relative energy to the main peak (ΔE) (eV), monopole intensity and main configurations of the O 1s satellite states of formaldehyde

| No. | Lunell et al.[a] | | | | This work | | | | | | |
| | Experimental | | CISD/INDO | | Experimental | | | SAC–CI general-R | | | |
	ΔE (eV)	Intensity	ΔE (eV)	Intensity	IP (eV)	ΔE (eV)	Intensity	IP (eV)	ΔE (eV)	Intensity	Main configurations[b] ($|C|>0.25$)
0	0.0	1.000	–	–	539.48	0.0	1.000	539.35	0.0	1.0000	$0.81\,(\mathrm{O}\,1s^{-1}) - 0.36\,(1b_1^{-1}\pi^*\mathrm{O}\,1s^{-1})$
1	–	–	–	–	549.18	9.7	0.005	549.05	9.70	0.0181	$0.79\,(\mathrm{O}\,1s^{-1}\pi^{*-1}\pi^{-1}) + 0.26\,(\pi^{-1}\pi^*\pi^{-1}\pi^*\,\mathrm{O}\,1s^{-1})$
2	12.2	0.043	9.62	0.073	551.68	12.2	0.030	551.36	12.01	0.1510	$0.77\,(\pi^{-1}\pi^*\,\mathrm{O}\,1s^{-1}) + 0.49\,(\pi^{-1}\pi^*\,\mathrm{O}\,1s^{-1}) - 0.41\,(\pi^{-1}\pi^{-1}\pi^{-1}\pi^*\,\mathrm{O}\,1s^{-1})$
3	–	–	14.45	0.007	554.18	14.7	0.003	554.49	15.14	0.0015	$0.54\,(\mathrm{O}\,1s^{-1}3b_2(\sigma^*)n^{-1}) + 0.42\,(n^{-1}\pi^*n^{-1}\pi^*\,\mathrm{O}\,1s^{-1})$
4	–	–	17.81	0.011	556.88	17.4	0.007	556.55	17.20	0.0181	$0.66\,(n^{-1}3b_2(\sigma^*)\,\mathrm{O}\,1s^{-1}) - 0.38\,(n^{-1}3b_2(\sigma^*)\pi^{-1}\pi^*\,\mathrm{O}\,1s^{-1}) - 0.30\,(n^{-1}3b_2(\sigma^*)\,\mathrm{O}\,1s^{-1})$
5	–	–	24.51	0.009	559.88	20.4	0.005	559.15	19.80	0.0025	$0.32\,(\mathrm{O}\,1s^{-1}6a_1(\sigma^*)5a_1(\sigma)^{-1}) + 0.29\,(\mathrm{O}\,1s^{-1}6a_1(\sigma^*)4a_1(\sigma)^{-1}) - 0.29\,(\mathrm{O}\,1s^{-1}3b_2(\sigma^*)n^{-1})$
								560.64	21.29	0.0033	$0.67\,(n^{-1}\pi^*\,\mathrm{O}\,1s^{-1}\pi^*n^{-1}) + 0.49\,(n^{-1}\pi^*\pi^{-1}3b_2(\sigma^*)\,\mathrm{O}\,1s^{-1}) + 0.33\,(5a_1(\sigma)^{-1}6a_1(\sigma^*)\,\mathrm{O}\,1s^{-1})$
								560.82	21.47	0.0044	$0.32\,(\mathrm{O}\,1s^{-1}6a_1(\sigma^*)5a_1(\sigma)^{-1}) + 0.32\,(\mathrm{O}\,1s^{-1}6a_1(\sigma^*)4a_1(\sigma)^{-1}) + 0.31\,(\pi^{-1}6a_1(\sigma^*)5a_1(\sigma)^{-1}\pi^*\mathrm{O}\,1s^{-1}) + 0.31\,(5a_1(\sigma)^{-1}\pi^*\,\mathrm{O}\,1s^{-1}6a_1(\sigma^*)\pi^{-1})$
								561.25	21.90	0.0027	$0.54\,(5a_1(\sigma)^{-1}6a_1(\sigma^*)\,\mathrm{O}\,1s^{-1})$
6	–	–	26.21	0.005	563.18	23.7	0.007	563.18	23.83	0.0016	$0.31\,(\pi^{-1}3p\,\mathrm{O}\,1s^{-1}) - 0.28\,(\mathrm{O}\,1s^{-1}\pi^*\pi^{-1}) + 0.27\,(\pi^{-1}\pi^*\pi^{-1}3p\,\mathrm{O}\,1s^{-1})$
								564.49	25.14	0.0016	$0.45\,(\mathrm{O}\,1s^{-1}3p\pi^{-1}) - 0.29\,(\pi^{-1}3p\mathrm{O}\,1s^{-1})$
								564.60	25.25	0.0072	$0.40\,(n^{-1}3p\,\mathrm{O}\,1s^{-1})$
7	–	–	26.59	0.026	567.48	28.0	0.005	564.92	25.57	0.0068	$0.32\,(5a_1(\sigma)^{-1}3s\,\mathrm{O}\,1s^{-1}) - 0.29\,(n^{-1}3p\mathrm{O}\,1s^{-1}) + 0.29\,(\mathrm{O}\,1s^{-1}3s5a_1(\sigma)^{-1})$
								565.16	25.81	0.0017	$0.38\,(4a_1(\sigma)^{-1}6a_1(\sigma^*)\,\mathrm{O}\,1s^{-1}) + 0.26\,(\mathrm{O}\,1s^{-1}6a_1(\sigma^*)4a_1(\sigma)^{-1}) + 0.28\,(\pi^{-1}3pn^{-1}\pi^*\,\mathrm{O}\,1s^{-1})$
								565.74	26.39	0.0089	$0.32\,(4a_1(\sigma)^{-1}6a_1(\sigma^*)\,\mathrm{O}\,1s^{-1}) + 0.27\,(\mathrm{O}\,1s^{-1}6a_1(\sigma^*)4a_1(\sigma)^{-1})$
								566.43	27.08	0.0059	$0.35\,(\pi^{-1}3b_2(\sigma^*)n^{-1}\pi^*\,\mathrm{O}\,1s^{-1}) + 0.27\,(\pi^{-1}\pi^*\,\mathrm{O}\,1s^{-1}) - 0.26\,(\mathrm{O}\,1s^{-1}\pi^*\pi^{-1})$
								567.28	27.93	0.0030	$0.34\,(5a_1(\sigma)^{-1}4s\,\mathrm{O}\,1s^{-1}) + 0.29\,(\mathrm{O}\,1s^{-1}4s5a_1(\sigma)^{-1})$

[a] Ref. [6].
[b] The spin functions of doubles (iaj) and triples ($iajbk$) are $\frac{1}{\sqrt{2}}(\alpha\beta - \beta\alpha)\alpha$ and $\frac{1}{2}(\alpha\beta - \beta\alpha)(\alpha\beta - \beta\alpha)\alpha$, respectively.

1s ionization are summarized in Table 3. As shown in Fig. 2, the experimental satellite spectrum is well reproduced by the SAC–CI calculation for both the peak positions and relative intensities, even though both of the orbital relaxation and correlation effect are larger for the O 1s ionization than for the C 1s ionization. Large deviations of the theoretical values from the experimental ones were reported for the ADC(4) calculations because of the significance of these effects [7].

Let us examine each of the seven bands: the assignments similar to the C 1s satellite spectrum are possible. Band 1 is characteristic because of its very small intensity in comparison with that of C 1s ionization. This band is observed at 9.7 eV as the shoulder of the strong band 2. The calculated energy is 9.70 eV relative to the main line and the pole strength is as small as 0.0181, in agreement with the experiment. This band was also calculated by the ADC(4) calculation: the predicted energy was 11.74 eV and the relative pole strength was 0.0002 [7]. The strongest band 2 is observed at 12.2 eV, while the SAC–CI method predicts the strong peak at 12.01 eV, in very good agreement with the experiment. Both bands 1 and 2 are characterized as $(\pi^{-1}\pi^*)$ transitions accompanying the O 1s ionization with some contribution of three-electron process, $(\pi^{-2}\pi^{*2})$ (see Table 3). The observed bands 1 and 2 have fine peak structures as in the case of the C 1s ionization; these structures are also attributed to the vibrational progression of the C–O stretching mode, since both states are characterized as a promotion of the π electron to the anti-bonding π^* orbital. It should be noted that the three-electron process, $(n^{-2}\pi^{*2})$, found in this region of the C 1s ionization is not found in the case of O 1s ionization. For analyzing this feature, the valence MO levels of the C 1s and O 1s ionized states were calculated with the ΔSCF method and are compared in Fig. 3. The n MO level of the C $1s^{-1}$ state is higher in energy than that of the O $1s^{-1}$ state because the n MO is localized at the oxygen atom. Therefore, the n–π^* energy separation is found to be larger in the O 1s ionized state than in the C 1s ionized state. Therefore, the $(n^{-2}\pi^{*2})$ state exists in the higher energy region in the O 1s spectrum than in the C 1s spectrum.
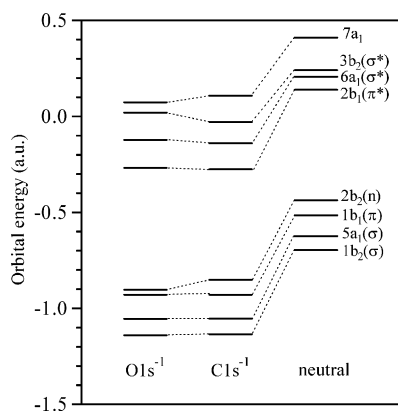
Band 3 is observed at 14.7 eV. Corresponding shake-up state would be valence $(n^{-1}3b_2(\sigma^*)) + (n^{-2}\pi^{*2})$ transition calculated at 15.14 eV from the shape of the satellite spectrum. Note an interesting mixing of the three-electron process $(n^{-2}\pi^{*2})$ in this satellite state. The next band 4 was previously assigned to the $(n^{-1}3b_2(\sigma^*))$ transition [6]. This band is observed at 17.4 eV in the present work and the shake-up state, which is also characterized as $(n^{-1}3b_2(\sigma^*))$ transition, is calculated at 17.20 eV with the large relative pole strength of 0.0181.

In the region of 19.80–21.90 eV, corresponding to band 5 centered at 20.4 eV, many shake-up states are predicted. As shown in Table 3, these shake-up states have the characters of the one-electron $(5a_1(\sigma)^{-1}6a_1(\sigma^*))$ and two-electron $(n^{-2}\pi^{*2})$ transitions. Band 6 is observed at 23.7 eV and the SAC–CI calculations attributed it to the shake-up states calculated at 23.83, 25.14, and 25.25 eV. These states are characterized mainly as Rydberg excitations accompanying the O 1s ionization. In this higher energy region, many shake-up states are calculated, though their intensities are quite small. Finally, in the energy region higher than $\sim$27 eV, a very broad band 7 is observed. This band was not reported in the previous works. This broad band is interpreted as the clusters of the shake-up states of small intensities calculated at 25.57, 25.81, 26.39, 27.08, and 27.93 eV. Their electronic structures are described in details in Table 3. There are three type transitions around band 7. The peaks whose energies are 25.57 and 27.93 eV are assigned to Rydberg $(5a_1(\sigma)^{-1}3s)$ and $(5a_1(\sigma)^{-1}4s)$ transitions, and the peaks at 25.81 and 26.39 eV are assigned to $(4a_1(\sigma)^{-1}6a_1(\sigma^*))$ transitions, and the peak at 27.08 eV is assigned to the three-electron process $(\pi^{-1}3b_2(\sigma^*)n^{-1}\pi^*)$.

5. Summary

The C 1s and O 1s satellite spectra of formaldehyde were measured with the high-resolution X-ray photoelectron spectroscopy. The details of the spectra were theoretically studied with the SAC–CI general-*R* method. The general-*R* method including triple and quadruple excitation *R* operators well described the multi-electron processes appearing as the satellite bands of the inner-shell photoelectron spectra; this theoretical method turned out to describe well both the orbital reorganizations and electron correlations accompanying the inner-shell ionizations. The peak positions and intensities of the satellite peaks were well predicted in comparison with the previous theoretical calculations.

The detailed assignments were given for the seven satellite peaks in the C 1s and O 1s ionization spectra and some of them were new interpretations. The satellite peaks were mainly attributed to the valence excitations accompanying the core-ionizations. The Rydberg excitations turned out to have small intensities. Many three-electron processes such as $n^{-2}\pi^{*2}$ and $\pi^{-2}\pi^{*2}$ were calculated in the low-energy region where valence shake-up states exist.

Fig. 3. Valence orbital levels of formaldehyde of O $1s^{-1}$ (ROHF), C $1s^{-1}$ (ROHF), and neutral (RHF).

Acknowledgement

References

[1] K. Siegbahn, C. Nordling, G. Johansson, J. Hedman, P.F. Heden, K. Hamrin, U. Gelius, T. Bergmark, L.O. Werme, R. Manne, Y. Baer, ESCA Applied to Free Molecules, North-Holland, Amsterdam, 1969.

[2] U. Gelius, J. Electron Spectrosc. Relat. Phenom. 5 (1974) 985.

[3] T.X. Carroll, T.D. Thomas, J. Electron Spectrosc. Relat. Phenom. 4 (1974) 270.

[4] H. Basch, Chem. Phys. 10 (1975) 157.

[5] I.H. Hiller, J. Kendrick, J. Electron Spectrosc. Relat. Phenom. 6 (1975) 325.

[6] S. Lunell, M.P. Keene, S. Svensson, J. Chem. Phys. 90 (1989) 4341.

[7] G. Angonoa, J. Schirmer, J. Mol. Struct. (THEOCHEM) 202 (1989) 203.

[8] H. Nakatsuji, K. Hirao, J. Chem. Phys. 68 (1978) 2053.

[9] H. Nakatsuji, Chem. Phys. Lett. 59 (1978) 362.

[10] H. Nakatsuji, Chem. Phys. Lett. 67 (1979) 329–334.

[11] H. Nakatsuji, Acta Chim. Acad. Sci. Hung. 129 (1992) 719.

[12] H. Nakatsuji, Computational Chemistry—Review of Current Trends, vol. 2, World Scientific, Singapore, 1997.

[13] H. Nakatsuji, Chem. Phys. 75 (1983) 425.

[14] H. Nakatsuji, J. Hasegawa, M. Hada, J. Chem. Phys. 104 (1996) 2321.

[15] H. Nakatsuji, J. Hasegawa, K. Ohkawa, Chem. Phys. Lett. 296 (1998) 499.

[16] H. Nakatsuji, Chem. Phys. Lett. 177 (1991) 331.

[17] H. Nakatsuji, J. Chem. Phys. 83 (1985) 731.

[18] H. Nakatsuji, J. Chem. Phys. 83 (1985) 5743.

[19] M. Ehara, H. Nakatsuji, Chem. Phys. Lett. 282 (1998) 347.

[20] M. Ehara, M. Ishida, K. Toyota, H. Nakatsuji, in: K.D. Sen (Ed.), Reviews in Modern Quantum Chemistry, World Scientific, Singapore, 2002, pp. 293–319.

[21] K. Kuramoto, M. Ehara, H. Nakatsuji, in press.

[22] R. Sankari, M. Ehara, H. Nakatsuji, Y. Senba, K. Hosokawa, H. Yoshida, A. De Fanis, Y. Tamenori, S. Aksela, K. Ueda, Chem. Phys. Lett. 380 (2003) 647.

[23] R. Sankari, K. Kuramoto, M. Ehara, and H. Nakatsuji, A. De Fanis, H. Aksela, S.L. Sorensen, M.N. Piancastelli, submitted for publication.

[24] H. Ohashi, E. Ishiguro, Y. Tamenori, H. Kishimoto, M. Tanaka, M. Irie, T. Tanaka, T. Ishikawa, Nucl, Instrum. Methods A 467–468 (2001) 529.

[25] K. Ueda, H. Yoshida, Y. Senba, K. Okada, Y. Shimizu, H. Chiba, H. Ohashi, Y. Tamenori, H. Okumura, N. Saito, S. Nagaoka, A. Hiraya, E. Ishiguro, T. Ibuki, I.H. Suzuki, I. Koyano, Nucl. Instrum. Methods A 467/468 (2001) 1502.

[26] Y. Tamenori, H. Ohashi, E. Ishiguro, T. Ishikawa, Rev. Sci. Instrum. 73 (2002) 1588.

[27] T. Tanaka, H. Kitamura, J. Synchrotron Radiat. 3 (1996) 47.

[28] Y. Shimizu, H. Ohashi, Y. Tamenori, Y. Muramatsu, H. Yoshida, K. Okada, N. Saito, H. Tanaka, I. Koyano, S. Shin, K. Ueda, J. Electron Spectrosc. Relat. Phenom. 114–116 (2001) 63.

[29] D.A. Mistrov, A. De Fanis, M. Kitajima, M. Hoshino, H. Shindo, T. Tanaka, Y. Tamenori, H. Tanaka, A.A. Pavlychev, K. Ueda, Phys. Rev. A 68 (2003) 022508.

[30] M. Hoshino, T. Tanaka, M. Kitajima, H. Tanaka, A. De Fanis, A.A. Pavlychev, K. Ueda, J. Phys. B: At. Mol. Opt. Phys. 36 (2003) L381.

[31] J.H. Callomon, E. Hirota, K. Kuchitsu, W.J. Lafferty, A.G. Maki, C.S. Pote, in: K.-H. Hellwege, A.M. Hellwege (Eds.), Landolt–Bornstein Numerical Data and Functional Relationships in Science and Technology, New Series, Group II, vol. 7, Springer-Verlag, Berlin, 1976.

[32] A. Shafer, H. Horn, R. Ahlrichs, J. Chem. Phys. 97 (1992) 2571.

[33] T.H. Dunning Jr., J. Chem. Phys. 90 (1989) 1007.

[34] T.H. Dunning Jr., P.J. Hay, in: H.F. Schaefer III (Ed.), Methods of Electronic Structure Theory, Plenum, New York, 1977.

[35] R.I. Martin, D.A. Shirley, J. Chem. Phys. 64 (1976) 3685.

[36] M.J. Frisch, G.W. Trucks, H.B. Schlegel, G.E. Scuseria, M.A. Robb, J.R. Cheeseman, J.A. Montgomery Jr., T. Vreven, K.N. Kudin, J.C. Burant, J.M. Millam, S.S. Iyengar, J. Tomasi, V. Barone, B. Mennucci, M. Cossi, G. Scalmani, N. Rega, G.A. Petersson, H. Nakatsuji, M. Hada, M. Ehara, K. Toyota, R. Fukuda, J. Hasegawa, M. Ishida, T. Nakajima, Y. Honda, O. Kitao, H. Nakai, M. Klene, X. Li, J.E. Knox, H.P. Hratchian, J.B. Cross, C. Adamo, J. Jaramillo, R. Gomperts, R.E. Stratmann, O. Yazyev, A.J. Austin, R. Cammi, C. Pomelli, J.W. Ochterski, P.Y. Ayala, K. Morokuma, G.A. Voth, P. Salvador, J.J. Dannenberg, V.G. Zakrzewski, S. Dapprich, A.D. Daniels, M.C. Strain, O. Farkas, D.K. Malick, A.D. Rabuck, K. Raghavachari, J.B. Foresman, J.V. Ortiz, Q. Cui, A.G. Baboul, S. Clifford, J. Cioslowski, B.B. Stefanov, G. Liu, A. Liashenko, P. Piskorz, I. Komaromi, R.L. Martin, D.J. Fox, T. Keith, M.A. Al-Laham, C.Y. Peng, A. Nanayakkara, M. Challacombe, P.M.W. Gill, B. Johnson, W. Chen, M.W. Wong, C. Gonzalez, J.A. Pople, Gaussian'03, Gaussian Inc., Pittsburgh, PA, 2003.

[37] K. Kuramoto, M. Ehara, K. Ueda, H. Nakatsuji, submitted for publication.